ARTICLE

Check for updates

Unveiling the properties of liquids via photothermal-induced diffraction patterns

Jorge L. Domínguez-Juárez [1,2 ✉], Rafael Quintero-Torres[1], Manuel A. Cardoso-Duarte[1], Mario A. Quiroz-Juárez [1], Jose L. Aragón[1] & Joel Villatoro [3,4 ✉]

The interaction of a laser with a liquid can cause temperature changes in the liquid from which some properties of the latter can be indirectly obtained. However, from just temperature changes, a sample cannot be identified. Here, we report on the interaction of tightly focused femtosecond infrared light into secondary hydrogen-bonded liquids like water, organic compounds, and binary mixtures. Such interaction induces a local change in the sample's index of refraction. The latter alters the wavefront of a white-light probe beam, giving rise to unique diffraction patterns that can be observed in the far field. The specific diffraction patterns may be considered as the optical signatures or fingerprints of the liquids studied. The technique proposed here is noninvasive and simple to implement with commercially available supercontinuum sources and digital cameras. Thus, it may be useful for the development of compact thermal lens spectroscopic instruments for a number of practical applications.

[1] Centro de Física Aplicada y Tecnología Avanzada, Universidad Nacional Autónoma de México, Juriquilla, Querétaro, México. [2] Cátedras CONACyT, Centro de Física Aplicada y Tecnología Avanzada, Universidad Nacional Autónoma de México, Juriquilla, Querétaro, México. [3] Department of Communications Engineering, University of the Basque Country UPV/EHU, Bilbao, Spain. [4] Ikerbasque-Basque Foundation for Science, Bilbao, Spain. ✉email: jldominguezju@conacyt.mx; agustinjoel.villatoro@ehu.eus

The interaction of laser light with known properties with polar or non-polar liquids has opened the door to investigate the linear and nonlinear thermal properties of liquids as well as stationary and time transient effects in them[1–3]. The laser-liquid interaction can cause temperature changes in the zone of the sample that interacts with the excitation laser beam. Hence, a laser-liquid interaction gives rise to a local inhomogeneous alteration of the sample's refractive index[4,5]. In liquids with a negative thermo-optic coefficient, the laser-exposed region can act as a negative lens that alters or deflects the optical path of a light beam that crosses such a region[6].

The *thermal* lens in pure liquids can deflect the same light beam that causes it; such deflection can be detected as intensity changes with a pinhole detector placed a few meters away from the sample[7,8]. The disadvantages in this case are the large dimensions and instability of the measuring setup. The thermal lens can also be analyzed with two laser beams with two different wavelengths; one is used as the excitation or pump beam and the other as the probe one[9–11]. In this case, the *thermal* lens gives rise to intensity changes of the probe beam that are easily monitored with a photodetector. The use of two different lasers entails critical alignment and increases the bulkiness of the setup, which may limit its practical applications[9,12].

From the intensity changes caused by the thermal lens, the optical and thermophysical properties of samples can be indirectly obtained[4,5,13]. Such properties include absorbance, density, thermo-optic coefficient, heat capacity, thermal conductivity, etc.[4,5,14,15]. For these reasons, the photothermal effect has multiple practical uses ranging from material characterization[16] to applications in biomedicine[17], in analytical chemistry[8], as well in lab-on-a-chip[14,18], in microscopy[19] and in thermoplasmonics[6,20].

In the vast majority of works reported in the literature, the intensity of the pump or probe beam is monitored as a function of time[7,10,11], position[17], or concentration[19]. From the time- or amplitude-dependent signals, the aforementioned physical and thermo-optic properties of a sample can be obtained. However, intensity changes are relative and do not depend exclusively on how much light was absorbed by a sample; they can also be affected by external factors or by the experimental conditions. This means, the photothermal lens technique cannot provide any data or information with which a sample or molecules can be identified. Thus, an approach or technique that is less sensitive to different experimental factors and that can provide a specific signature about the sample is highly desirable to expand the use of the photothermal lens phenomenon.

Here, we report on the observation of diffraction patterns when a secondary hydrogen-bonded liquid was exited with a femtosecond laser emitting at 1040 nm, and it was probed with multiple wavelengths, more specifically, with supercontinuum visible light, i.e. in the 500–800 nm wavelength range. We observed diffraction patterns whose topology and geometry may be correlated with the spatial physicochemical characteristics of a liquid. The diffraction patterns were captured with an inexpensive digital camera and processed with a simple digital spatial Fourier filter.

The technique reported here allowed us to observe well-defined diffraction patterns from water, colorless organic compounds, and binary mixtures. The diffraction patterns may provide a fingerprint or an 'optical signature' of the thermal lens effect in such liquids. Our technique can be implemented with commercially available supercontinuum light sources and compact digital cameras. Therefore, the approach reported here can pave the way to the development of compact *thermal* lens instruments for a variety of practical applications.

Results

Generation of supercontinuum light. To generate supercontinuum visible light (from 500 to 800 nm), a 330-femtosecond Gaussian laser beam (Spirit One, Spectra Physics) emitting at 1040 nm was focused in a sapphire crystal. The visible light had very low intensity; the average power was approximately 0.427 mW. The infrared femtosecond laser, whose average power was 107 mW, was also used as the excitation (pump) beam to the samples. The generated visible light was used as the probe beam. After the interaction with the sapphire crystal, the pump beam was focused into the liquid sample, which was in a 1-cm wide quartz cell. The probe beam was also focused into the liquid to sample the region that was exposed to the pump infrared beam, see Fig. 1. Before the interaction with the sample, both the pump and probe beams were linearly polarized. The probe infrared beam was cut off before reaching the camera with a suitable filter. The quartz cell was placed perpendicular to the pump and probe beams, and the focal point was approximately in the middle of the sample cell.

It is known that femtosecond infrared laser pulses tightly focused into a liquid induce different effects that depend on the type of liquid. The laser pulses can induce transient pressure waves or localized heat in the liquid[5,11,21], which generate a particular refractive index gradient around the focal point. The localized refractive index alteration in the liquid deflects or changes the phase of the probe beam. Such deflection or phase changes give rise to time-dependent intensity changes of the probe beam that can be monitored with a fast photodetector. From such intensity changes, radiation forces[22], pressure waves[21], or molecular interactions[10] in a liquid can be detected or studied.

Diffraction patterns. We have found that the changes in the sample produced by its exposure to focused femtosecond laser pulses can be analyzed by means of diffraction patterns. The latter were generated by the multiple wavelengths of the supercontinuum light that probed the region of the liquid exposed to infrared laser pulses. The diffraction patterns were easily observed and captured with an inexpensive digital camera (EOS-M50) whose maximum speed was 24 frames per second.

In Fig. 2, we show the observed diffraction patterns when the samples were water, methanol, ethanol, and 1-propanol. All the diffraction patterns were monitored in all cases under the same experimental conditions; the optical power of the infrared beam was 107 mW. In the figure, the blue images are the digital spatial Fourier transforms of the intensity-transformed grayscale photographs of the diffraction patterns. It can be observed that the diffraction patterns and the corresponding digital Fourier transforms are different for each sample. This suggests that a photothermal-induced diffraction pattern may be considered as the 'optical signature' of a sample. This means, the technique reported here can eventually be used to identify a liquid sample in
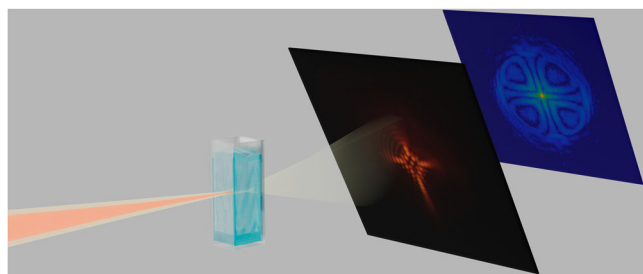
Fig. 1 Schematic of the experimental set-up used for observing diffraction patterns (first photograph) generated in femtosecond laser-exposed liquids placed in a quartz cell. The blue image is the digital Fourier transform of the photograph.
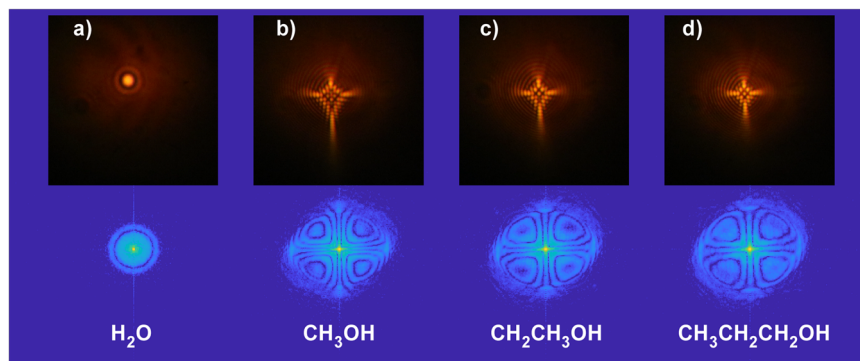
Fig. 2 The top images are photographs of the diffraction patterns observed when the samples were a) water, b) methanol, c) ethanol, and d) 1-propanol. All the photographs were captured with an EOS-M50 Cannon camera. The bottom blue images are the corresponding spatial digital Fourier transforms of the photographs.
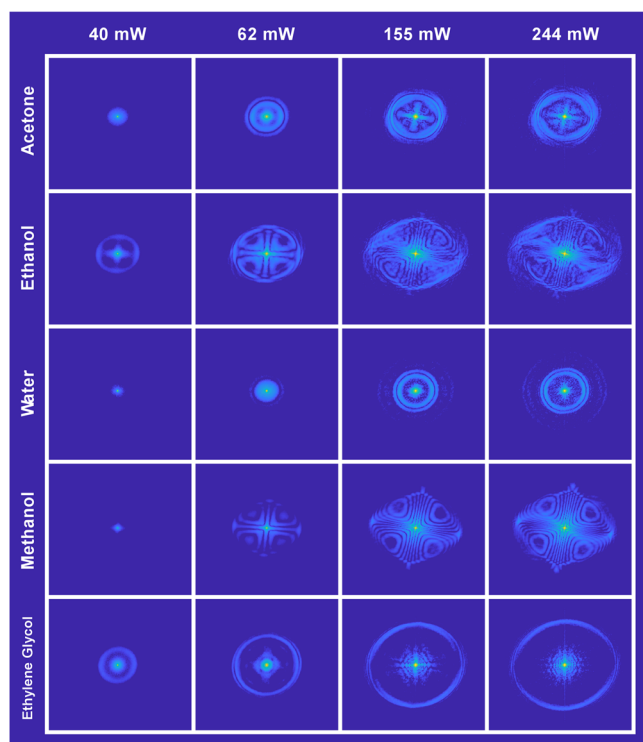
Fig. 3 Digital Fourier transforms calculated from the diffraction patterns generated by colorless solvents for different optical powers of the pump laser beam. From top to bottom, the liquids were acetone, ethanol, water, methanol, and ethylene glycol.

a similar manner that the diffraction of X-rays from crystals are used to identify them.

The effect of the optical power of the pump infrared beam on the diffraction patterns was investigated. In this case, the pump and probe beams were focused into the sample as mentioned above; the optical power of the pump laser was varied from 40 to 244 mW. The generated supercontinuum visible light was used as the probe light in all cases.

The observed logarithmic spatial Fourier transform (SFT) of the intensity grayscale digital images, when the liquids were acetone, ethanol, water, methanol, and ethylene glycol are shown in Fig. 3. Note from the figure that the shape of the patterns depends on the power of the excitation laser. However, for a pump power higher than 155 mW, the pattern of each studied sample was no longer altered. Note also that for such a pump power, the diffraction pattern generated by each sample is unique.

The pattern generated by water is circular and is completely different from those generated by other colorless organic compounds.

The results shown in Fig. 3 indicate that the localized refractive index changes of our samples depended on the intensity of the pump laser; which is in agreement with the temperature-dependent phase shift reported in[23,24]. It also depended on the type of liquid, hence, on its optical properties. The results shown in Fig. 3 also suggest that there is a minimum pump power that can be used to obtain the 'optical signature' of a sample. In our case, it was above 60 mW of average power. Such low power is easy to reach in an infrared laser.

We studied the effect of a convergent and divergent pump beam on the samples; this means the focal point of the pump and probe beams were after or before the sample. To do so, we displaced the sample cell to different positions. In all cases, the optical power of the pump beam was fixed (90 mW). Figure 4 displays the 'optical signatures' that were observed in two liquids (water and ethanol). The figure shows five diffraction patterns, and their corresponding spatial Fourier transforms. For comparison, the patterns observed when the pump beam was focused into the sample are also shown. It can be observed that the diffraction patterns are completely different when the pump infrared beam was convergent, divergent, or focused into the sample.

The patterns shown in Fig. 4 agree well with the results reported in Ref. [25]. When the pump beam was divergent, the central zone of the diffraction patterns had a dark zone. However, when the pump beam was convergent, the central zone of the diffraction patterns was bright. According to Ref. [25] the change from dark to bright zones is due to the effect of an additional phase shift caused by the refractive index change on the far-field diffraction pattern.

Label-free experiments with colorless binary mixtures of alcohol and water were also carried out. In all cases, the experimental conditions were the same. The volume of each mixture was constant; 1 ml. The results of our experiments are summarized in Fig. 5. The figure shows the spatial Fourier transforms of the digital images of the observed diffraction patterns (photographs not shown) of methanol, ethanol, and 1-propanol with different molar fractions of water ranging from 0.25 to 0.9. Note that as the molar fraction of water decreases, the patterns evolve from rings of different diameters to more complex shapes that cannot be perceived with the naked eye. Thus, to calculate the percentage of water in an alcohol, hence, the amount of a solute in a solvent with the technique reported here, a digital image analysis is necessary. In the following paragraphs, we will show how such an analysis can be carried out. The results shown

here allow studying alcohol-water binary mixtures by using the thermal technique in a different manner than that reported until now[9–12,16,21–23,26–30].

Discussion

All the liquids studied here are secondary hydrogen-bonded ones. Femtosecond infrared laser pulses in such liquids generate a radial heat flow that is dissipated from the center of the pump beam to the surroundings[31–33]. Therefore, a local temperature, hence, a local refractive index gradient is formed in the sample[2,23,34,35]. The region of the liquid with a varying refractive index diffracts the focused white light beam that propagates collinearly with the pump beam. As shown in the above figures, the shape of the diffraction patterns is unique for each liquid or mixture that was studied.
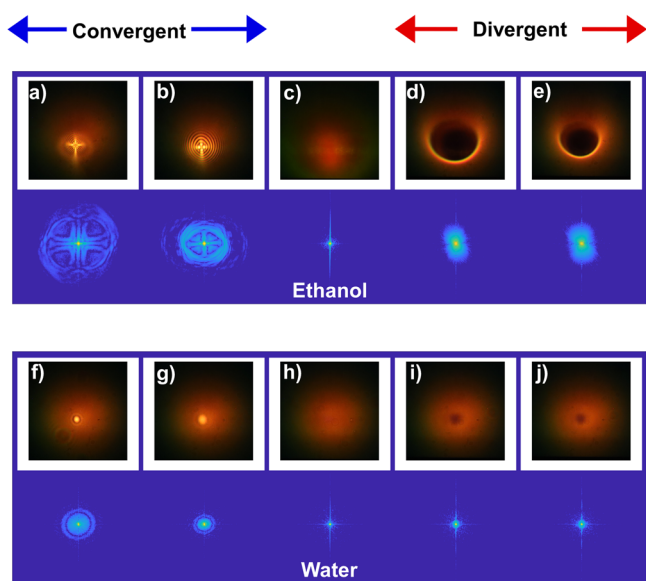
Fig. 4 Results obtained when the pump infrared beam was convergent, focused, or divergent into the sample. Diffraction patterns and their spatial Fourier transforms (blue images) shown in **a–e** were obtained when the sample was ethanol. The patterns shown in **f–j** were obtained when the sample was water.
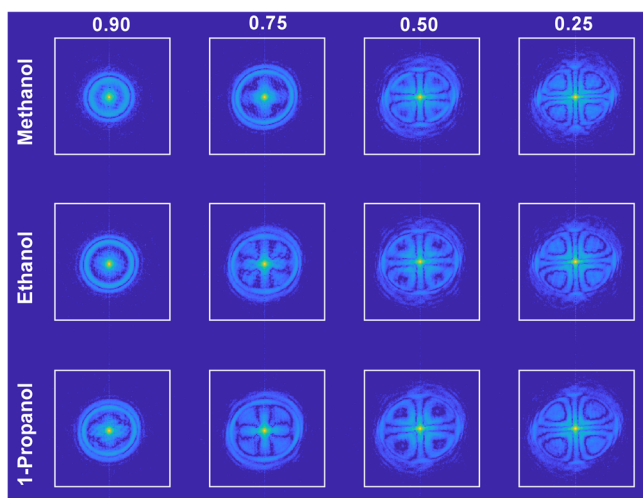
Fig. 5 Digital Fourier transforms of binary mixtures; methanol, ethanol, and 1-propanol with water. The top values are the molar fractions of water in the alcohols.

In a homogenous medium, the temperature-dependent phase shift of the probe beam can be expressed as $\triangle\phi(x,y) = kL(\partial n_l/\partial T)T(x,y)$, where k is the infrared wave number in the solvent, L is the length of the quartz cell that contained the liquid, and T is the stationary temperature profile in the sample[23,24,36]. The temperature-dependent change in the refractive index of the liquid is $\partial n_l/\partial T$[37,38].

The radial index of refraction in the liquid produced by the pump laser beam can be expressed as $n_l = n_0 + \delta n_l(r_s, z)$, where n_0 is the average refractive index of the liquid[3] and $\delta n_l(r_s, z)$ is the three-dimensional change of the index of refraction in the sample. In the above expression, z is the direction of propagation of the pump and probe beams and r_s is the radial direction that is perpendicular to the z-direction. Such alteration of the refractive index in the sample deflects each ray of the probe beam. The angle of deflection can be expressed as:

$$\theta_l = \frac{\partial}{\partial r_s}\left|\int_0^L \frac{\delta n_l(r_s, z)}{n_0}\right| \quad (1)$$

We can assume that the sample with the same light-liquid interaction L and the spatial Fourier transform of the digital image from the observed diffraction patterns make θ_l independent of z. The diffraction patterns were projected on a screen located at 28 cm from the sample cell, and they were photographed with the digital camera mentioned above. The pixel dimensions, width and height on an image were marked with two axes: x_p and y_p in pixels units. Thus, the area of each digital photograph was $A_p = (x_p \times y_p)$.

First, we obtained the red-green-blue (RGB) matrix of each image from each color photograph of the far-field diffraction patterns. Such a matrix can be expressed with color including c_P as $A_{p-bits}^{RGB}[x_p, y_p, c_P]$. From the non-saturated pixel intensity RGB images, we obtained the grayscale images of each diffraction pattern. Each matrix in this case can be expressed as $A_{p\_0\_255}^{gray}[x_p, y_p]$.

The grayscale images allowed us to calculate the spatial distribution intensity information of each sample. The pixel intensity in the logarithmic scale was obtained with an imaging process tool (MATLAB Image Processing Toolbox). From such intensities, the digital Fourier transforms, whose matrices can be expressed as $\Theta_l[x_p, y_p]$, of each diffraction pattern were calculated. The digital Fourier transforms allowed us to extract the periodicity of the spatial phase variations from the pixel intensity distribution of each diffraction pattern. Thus, the logarithmic grayscale pixel intensity denoted as $I_l^p(r_s, \theta_l)$, contained a radial distribution of the diffraction patterns.

To distinguish one liquid from another or to calculate the percentage of a solvent in a solution, see Fig. 5, we integrated the pixel polar deflection intensity from the central value of the image ($r_s = 1$) to the maximum size of such an image ($r_s = r_i$). This means a change of coordinates from r_s to R

$$I_l^{\theta,r}(R, \theta_l) = \int_1^{r_i} I_l^p(r_s, \theta_l)dr_s \quad (2)$$

To analyze the patterns shown in Fig. 5, the radial pixel intensity distribution $I_l^{\theta,r}(R, \theta_l)$ given in Eq. (2) as a function of the molar fraction of water x_{H_2O} was calculated for each mixture. Some of these calculations are shown graphically in Fig. 6.

To interpret the results shown in Fig. 6 we carried out the following analysis. The density of water, methanol, ethanol, and 1-propanol, are well known. These are respectively, 0.997, 0.792, 0.789, and 0.803 g/mL. These values were taken from the supplier and literature[39]. As the total volume of the mixtures was constant (1 mL) in all cases, thus, the mass in such a volume depended on the liquids that composed the mixture. We can use a total relative
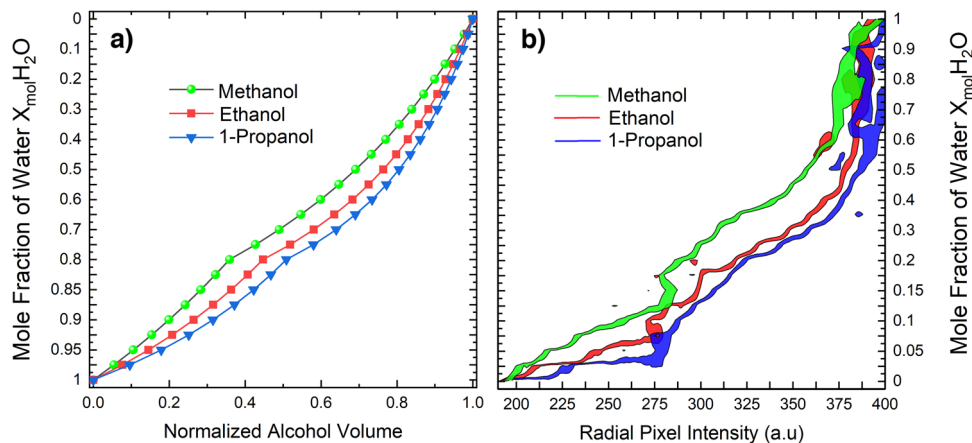
Fig. 6 Analysis of the molar fraction of water to distinguish some liquids. a Molar fraction of water as a function of **a** the normalized volume and **b** radial pixel intensity of methanol, ethanol, and 1-Propanol.

volume (V_{Tw}) with respect to the density of water (ρ_w) as $V_{Tw} = m_{Tm}/\rho_w$, where m_{Tm} is the total mass of the mixture. This relative volume can be normalized from 0 to 1 from a minimum value ($V_{TRw\min}$), which corresponds when the sample is a pure alcohol. Therefore, the normalized volume with respect to water for 1 mL of volume is:

$$V_{TRw} = \frac{V_{Rw} - V_{TRw\min}}{1 - V_{TRw\min}} \qquad (3)$$

The value given by Eq. (3) can be correlated with the values of deflection of the light rays that are obtained from the molar fractions of water. It can be observed in Fig. 6 that there is an increment in the intensity of the radius of deflection of the digital diffraction patterns with respect to the normalized volume. This means that we can find the mass of a mixture by using this expression: $m_{TM} = (\rho_w)(V_{NRw})(1mL)$. In other words, from the digital diffraction patterns, we can calculate the mass of a solvent in a solution provided that the density of water is known and used as a reference.

The most important differentiator enabled by the technique reported here arise from the possibility of visualizing well-defined diffraction patterns with a conventional digital camera. Simple image processing allowed us to obtain images whose topology and geometry were different when the sample was water, pure alcohol or organic compound, and even binary mixtures. The results reported here suggest that the diffraction patterns may represent an optical fingerprint or signature, which must be associated with the physicochemical properties of the liquids and even with their molecular dynamics. However, to calculate such properties or to study such molecular dynamics, a detailed mathematical model that relates the shape of the diffraction patterns with the refractive index changes in the laser-exposed zone is necessary.

Conclusions
In conclusion, in this work, we have reported on a technique to visualize diffraction patterns that were generated when focused femtosecond laser pulses interacted with a transparent liquid. We observed diffraction patterns that were different for each liquid studied. Such diffraction patterns were generated by a region of the liquid with varying refractive index due to its exposure to the pump femtosecond laser beam.

The visualization and analysis of the diffraction patterns may be an alternative to the typical relative and non-specific time- or amplitude-dependent signals monitored in conventional thermal lens spectroscopy. For example, we monitored the diffraction patterns with an inexpensive low-speed digital camera. To analyze

the patterns, a simple image processing was used, which entailed the conversion of color images to grayscale and a spatial Fourier transform. Our results suggest that the digital Fourier image of a sample can be considered as its optical signature or fingerprint; thus, it seems feasible to differentiate one liquid (sample) from another; also, if it is pure or it is mixed with another one.

The technique and results reported here can be useful in different applications of practical interest, for example, to study the relevance of secondary hydrogen bonding in thermal dissipation in polar liquids. Water is the main component of biological organisms whereas alcohols are important in the chemical industry. Moreover, hydrogen bonding occurs in different polymers, DNA, or proteins. Thus, our results may be useful in diverse areas. An important advantage of the technique reported in this work is that it can be implemented with commercially available supercontinuum sources and miniature digital cameras. Thus, compact measuring instruments can be developed, the same that can be used in point-of-need tests.

References
1. Gordon, J. P., Leite, R. C. C., Moore, R. S., Porto, S. P. S. & Whinnery, J. R. Long-transient effects in lasers with inserted liquid samples. *J. Appl. Phys.* **36**, 3–8 (1965).
2. Callen, W. R., Huth, B. G. & Pantell, R. H. Optical patterns of thermally self-defocused light. *Appl. Phys. Lett.* **11**, 103–105 (1967).
3. Dabby, F. W., Gustafson, T. K., Whinnery, J. R., Kohanzadeh, Y. & Kelley, P. L. Thermally self-induced phase modulation of laser beams. *Appl. Phys. Lett.* **16**, 362–365 (1970).
4. Proskurnin, M. A. et al. Advances in thermal lens spectrometry. *J. Anal. Chem.* **70**, 249–276 (2015).
5. Proskurnin, M. A. et al. Photothermal and optoacoustic spectroscopy: state of the art and prospects. *Phys.-Uspekhi* **65**, 270–312 (2022).
6. Baffou, G.; Quidant, R. Thermoplasmonics. In *World Scientific Handbook of Metamaterials and Plasmonics*, https://doi.org/10.1142/9789813228726_0010 379-407.
7. Silva, R. et al. Thermal lens spectrometry: optimizing amplitude and shortening the transient time. *AIP Adv.* **1**, 022154 (2011).
8. Franko, M. & Tran, C. D. Analytical thermal lens instrumentation. *Rev. Sci. Instrum.* **67**, 1–18 (1996).

9. Long, M. E., Swofford, R. L. & Albrecht, A. C. Thermal lens technique: a new method of absorption spectroscopy. *Science* **191**, 183–185 (1976).
10. Rawat, A. K., Chakraborty, S., Mishra, A. K. & Goswami, D. Unraveling molecular interactions in binary liquid mixtures with time-resolved thermal-lens-spectroscopy. *J. Mol. Liq.* **336**, 116322 (2021).
11. Capeloto, O. A. et al. Nanosecond pressure transient detection of laser-induced thermal lens. *Appl. Opt.* **59**, 3682–3685 (2020).
12. Swofford, R. L., Long, M. E. & Albrecht, A. C. C–H vibrational states of benzene, naphthalene, and anthracene in the visible region by thermal lensing spectroscopy and the local mode model. *J. Chem. Phys.* **65**, 179–190 (1976).
13. Franko, M. & Tran, C. D. Thermal lens spectroscopy. In *Encyclopedia of Analytical Chemistry*, https://doi.org/10.1002/9780470027318.a9079.
14. Chen, C., Shimizu, H. & Kitamori, T. Review of ultrasensitive readout for micro-/nanofluidic devices by thermal lens microscopy. *J. Opt. Microsyst.* **1**, 020901 (2021).
15. Kitamori, T. Thermal lens microscope and microchip chemistry. *Bull. Chem. Soc. Jpn* **92**, 469–473 (2019).
16. Singhal, S. & Goswami, D. Thermal lens study of NIR femtosecond laser-induced convection in alcohols. *ACS Omega* **4**, 1889–1896 (2019).
17. Pleitez, M. A. et al. Photothermal deflectometry enhanced by total internal reflection enables non-invasive glucose monitoring in human epidermis. *Analyst* **140**, 483–488 (2015).
18. Shimizu, H., Chen, C., Tsuyama, Y., Tsukahara, T. & Kitamori, T. Photothermal spectroscopy and micro/nanofluidics. *J. Appl. Phys.* **132**, 060902 (2022).
19. Adhikari, S. et al. Photothermal microscopy: imaging the optical absorption of single nanoparticles and single molecules. *ACS Nano* **14**, 16414–16445 (2020).
20. Baffou, G. et al. Thermal imaging of nanostructures by quantitative optical phase analysis. *ACS Nano* **6**, 2452–2458 (2012).
21. Capeloto, O. A. et al. Induction and detection of pressure waves by pulsed thermal lens technique in water–ethanol mixtures. *Appl. Opt.* **60**, 4029–4033 (2021).
22. Astrath, N. G. C. et al. Unveiling bulk and surface radiation forces in a dielectric liquid. *Light.: Sci. Appl.* **11**, 103 (2022).
23. Dominguez-Juarez, J. L. et al. Influence of solvent polarity on light-induced thermal cycles in plasmonic nanofluids. *Optica* **2**, 447–453 (2015).
24. Domínguez-Juárez, J. L., Quiroz-Juárez, M. A., Aragón, J. L., Quintero-Bermúdez, R. and Quintero-Torres, R. Complete numerical description of the laser-induced thermal profile in a liquid, to explain complex self-induced diffraction patterns. *arXiv* (2022), 10.48550/ARXIV.2208.06489, https://doi.org/10.48550/ARXIV.2208.06489.
25. Sigel, R., Fytas, G., Vainos, N., Pispas, S. & Hadjichristidis, N. Pattern Formation in Homogeneous Polymer Solutions Induced by a Continuous-Wave Visible Laser. *Science* **297**, 67–70 (2002).
26. Mialdun, A. et al. A comprehensive study of diffusion, thermodiffusion, and Soret coefficients of water-isopropanol mixtures. *J. Chem. Phys.* **136**, 244512 (2012).
27. Häbich, A., Ducker, W., Dunstan, D. E. & Zhang, X. Do Stable Nanobubbles Exist in Mixtures of Organic Solvents and Water? *J. Phys. Chem. B* **114**, 6962–6967 (2010).
28. Bosch, E. et al. Solute-solvent and solvent-solvent interactions in binary solvent mixtures. 2. Effect of temperature on the ET(30) polarity parameter of dipolar hydrogen bond acceptor-hydrogen bond donor mixtures. *J. Phys. Org. Chem.* **9**, 403–410 (1996).
29. Buhvestov, U., Rived, F., Ràfols, C., Bosch, E. & Rosés, M. Solute–solvent and solvent–solvent interactions in binary solvent mixtures. Part 7. Comparison of the enhancement of the water structure in alcohol–water mixtures measured by solvatochromic indicators. *J. Phys. Org. Chem.* **11**, 185–192 (1998).
30. Ventura, M., Silva, J. R., Catunda, T., Andrade, L. H. C. & Lima, S. M. Identification of overtone and combination bands of organic solvents by thermal lens spectroscopy with tunable Ti:sapphire laser excitation. *J. Mol. Liq.* **328**, 115414 (2021).
31. Anthore, R., Flament, P., Gouesbet, G., Rhazi, M. & Weill, M. E. Interaction between a laser beam and some liquid media. *Appl. Opt.* **21**, 2–4 (1982).
32. Gusev, V., Picart, P., Mounier, D. & Breteau, J. M. On the possibility of ultrashort shear acoustic pulse excitation due to the laser-induced electrostrictive effect. *Opt. Commun.* **204**, 229–236 (2002).
33. Gouesbet, G., Weill, M. E. & Lefort, E. Convective and free surface instabilities provoked by heating below an interface. *AIAA J.* **24**, 1324–1330 (1986).
34. Leite, R. C. C., Moore, R. S. & Whinnery, J. R. Low absorption measurements by means of the thermal lens effect using an He–Ne laser. *Appl. Phys. Lett.* **5**, 141–143 (1964).
35. Shrestha, S., Dominguez-Juarez, J. L. & Vuong, L. T. Light-induced electrohydrodynamic instability in plasmonically absorbing gold nanofluids. *Phys. Rev. Fluids* **2**, 064201 (2017).
36. Garcia Ramirez, E. V. et al. Z-scan and spatial self-phase modulation of a Gaussian beam in a thin nonlocal nonlinear media. *J. Opt.* **13**, 085203 (2011).
37. Nascimento, C. M. et al. Experimental demonstration of novel effects on the far-field diffraction patterns of a Gaussian beam in a Kerr medium. *J. Opt. A: Pure Appl. Opt.* **8**, 947–951 (2006).
38. González, B., Calvar, N., Gómez, E. & Domínguez, Á. Density, dynamic viscosity, and derived properties of binary mixtures of methanol or ethanol with water, ethyl acetate, and methyl acetate at T=(293.15, 298.15, and 303.15)K. *J. Chem. Thermodyn.* **39**, 1578–1588 (2007).

Author contributions

J.L.D.J. has conceived the project; J.L.D.J., R.Q.T., and M.A.C.D. designed and implemented the experimental setup and methodology; J.L.D.J., R.Q.T., M.A.C.D, M.A.Q.J, J.L.A., and J.V. contributed to the planning and discussion of this study; validation: J.L.D.J., R.Q.T., M.A.C.D., M.A.Q.J., J.L.A., and J.V; formal analysis: J.L.D.J., R.Q.T. M.A.C.D, J.L.A., and J.V; investigation: J.L.D.J., R.Q.T., M.A.C.D., M.A.Q.J., J.L.A., and J.V.; resources: J.L.D.J., R.Q.T., J.L.A., and J.V.; data curation: J.L.D.J., R.Q.T., M.A.C.D., J.L.A., and J.V.; writing—original draft preparation: J.L.D.J., and J.V.; writing—review and editing: J.L.D.J., R.Q.T., M.A.C.D., M.A.Q.J., J.L.A., and J.V.; visualization: J.L.D.J., and J.V.; project administration: J.L.D.J., R.Q.T., J.L.A., and J.V.; funding acquisition: J.L.D.J., R.Q.T., M.A.Q.J., J.L.A., and J.V. All authors have read and agreed to the published version of the manuscript.

Competing interests

The authors declare no competing interests.

Additional information

Supplementary information The online version contains supplementary material available at https://doi.org/10.1038/s42005-023-01278-x.

Correspondence and requests for materials should be addressed to Jorge L. Domínguez-Juárez or Joel Villatoro.

Peer review information *Communications Physics* thanks Hisashi Shimizu and the other, anonymous, reviewer(s) for their contribution to the peer review of this work. A peer review file is available.

Reprints and permission information is available at http://www.nature.com/reprints

Publisher's note Springer Nature remains neutral with regard to jurisdictional claims in published maps and institutional affiliations.